

# Two Dimensional Finite Element Method-Based Simulation of the Brownian Motion of a Spherical Particle in Water

Katarina Radulović and Sylvia Jeney

**Abstract**—One of the most attractive experimental methods for measuring the forces starting in the subnano range is photonic force microscopy (PFM). A proper use of the PFM is based on tracking movements of test particles in a given environment that is essentially Brownian. Brownian motion of test particles can be used for calibration and for determination of viscoelastic parameters of the environment. Our goal is to determine the two-dimensional mean square displacement (MSD) of a spherical silica particle in water which is subject to random thermal forces. The problem is modeled and simulated in commercial software package ANSYS 12.1-Mechanical APDL.

**Index Terms**—Brownian motion, finite element method modeling, optical tweezers, particle tracking, photonic force microscopy.

## I. INTRODUCTION

THE Atomic Force Microscope (AFM) was considered to be the ideal tool for physical studies of live biological specimens. However, the rough surface of a cell often prevents the tip of a mechanical cantilever from following the fine topographic details. Furthermore, forces of several tens of piconewtons can deform soft cellular structures, such as the plasma membrane. Therefore, a scanning probe microscope without a mechanical contact, which works with extremely small loading forces, is desirable. Such an instrument, the Photonic Force Microscope (PFM), has been developed at the European Molecular Biology Laboratory (EMBL) in Heidelberg ten years ago [1]. This three-dimensional scanning probe technique is based on optical tweezers (OT), scientific manipulation technique that uses a highly focused laser beam to provide an attractive or repulsive force to physically hold and move small objects [2]. Small objects like nano-particles, living cells, bacteria and viruses in physiological solution can be manipulated and positioned in 3D with a precision of a few

nanometers [3]. Compared with AFM techniques, the mechanical cantilever of the AFM is replaced with optical tweezers and the cantilever tip by a trapped bead. The optical forces generated by an OT are typically in the piconewton range, making it an ideal tool for studying the mechanics of individual molecules. In the same time, an optically trapped dielectric particle acts as a probe, which, driven by thermal noise (Brownian motion), scans its local environment in a volume determined by the optical trap. In that way, the viscoelastic parameters of the environment can be obtained. This approach, called microrheology, typically measures the mean square displacement (MSD) of the Brownian particle. The optical trap is taken to be a potential well with a stiffness  $k$ , controlled by the power of a laser beam. The proper use of PFM (precisely, the proper interpretation of experimental results) needs a calibrated optical trap, that is, a precisely defined stiffness constant  $k$ . There are several ways to do this, and all of them involve the observation of the bead's Brownian motion, while it is in the trap's potential well [4]. Those are the reasons why it is so important to know the parameters of the Brownian particle's trajectory. The main problem in Brownian movement monitoring is that due to the small trapping force constants, thermal position fluctuations of the probe are relatively large in comparison to the thermal motion of an AFM cantilever. So, the three-dimensional position of the bead must be measured with a spatial and temporal resolutions in the nanometre and microsecond range, respectively.

The Brownian motion is an erratic-type motion, carried out by a particle immersed in a fluid under the effect of the collisions it undergoes with the molecules of the fluid. The origin of the random motion was first successfully explained by Einstein as the amplification of the statistical fluctuations of the surrounding fluid molecules. Since then, the theory of Brownian motion has found broad applications in the description of phenomena in many fields in science and even in financial models. Due to the fractal nature of a diffusive Brownian particle's trajectory, the length of the path traveled in a given time interval is unknown. Therefore, the particle's velocity is ill-defined, leading to confusion in early attempts to connect the particle's apparent velocity to the temperature as demanded by the equipartition theorem [5]. The mean square

K.R. wishes to acknowledge funding by the Serbian Ministry of Education and Science through the project TR 32008. Some results of this paper were presented at 55<sup>th</sup> ETRAN Conference, Banja Vrućica, June 6-9, 2011.

K. Radulović is with the ICTM – Center of microelectronic technologies and single crystals, Njegoševa 12, 11000 Belgrade (email: kacar@nanosys.ihtm.bg.ac.rs).

S. Jeney is with the Institut de Physique de la Matière Complexe, Ecole Polytechnique Fédérale de Lausanne (EPFL), CH-1015 Lausanne, Switzerland.

displacement (MSD), on the other hand, can be measured and it was shown by Einstein to increase linearly with time  $t$ :  $\langle [x(t)]^2 \rangle = 2dDt$ , where  $\langle [x(t)]^2 \rangle$  is the mean square displacement (MSD) in one dimension of a free Brownian particle during time  $t$ ,  $d$  is dimensionality, and  $D$  is the diffusion constant. The diffusion constant can be calculated by  $D = k_B T / \gamma$ , where  $k_B$  is Boltzmann's constant,  $T$  is the temperature, and  $\gamma$  is the Stokes viscous drag (friction) coefficient.

This stochastic description of the interactions of the particle with the surrounding fluid must break down at short timescales, where the particle's inertia becomes significant. In the inertia-dominated regime, termed ballistic, the particle's autocorrelation function has a peak. Loosely speaking, after receiving an impulse from the surrounding fluid molecules, the particle flies in a straight line with constant velocity before collisions with fluid molecules slow it down and randomize its motion.

In the ballistic regime the MSD approaches  $(k_B T / m) t^2$  below the momentum relaxation time of a particle with mass  $m$ ,  $\tau_p = m / \gamma$ . Because of the lower viscosity of gas, compared with liquid, the  $\tau_p$  of a particle in air is much larger. This lowers the technical demand for both temporal and spatial resolution for measurements in a gas environment. The main difficulty of performing high-precision measurements of a Brownian particle in air, however, is that the particle will fall under the influence of gravity. This problem could be overcome by using optical tweezers to simultaneously trap and monitor a silica bead in air and vacuum, allowing long-duration, ultra-high-resolution measurements of its motion. Some recent simulations as well as experiments showed that, even for timescales much larger than  $\tau_p$ , there are deviations from random diffusive behavior, originating from the inertia of the surrounding fluid, which leads to long-lived vortices caused by and in turn affecting the particle's motion [6]. These hydrodynamic memory effects introduce an intermediate regime between the purely ballistic  $\sim t^2$  and the diffusive  $\sim 2Dt$  scaling, where the MSD takes on a rather complicated form.

In addition, the correct hydrodynamic treatment modifies the MSD in the ballistic regime to  $(k_B T / m^*) t^2$ , where  $m^*$  is an effective mass given by the sum of the mass of the particle and half the mass of the displaced fluid.

The equation that successfully describes the probe motion over entire time domain is the classical phenomenological Langevin' equation. For the sake of simplicity, the one-dimensional Langevin equation is discussed:

$$m \frac{d^2 x}{dt^2} = -\gamma \frac{dx}{dt} + F(t) + F_{ext}(t) \quad (1)$$

We associate a coordinate  $x$  with the Brownian particle's position. Two forces, both characterizing the effect of the fluid, act on the particle of mass  $m$ : a viscous friction force  $-\gamma(dx/dt)$ , characterized by the friction coefficient  $\gamma > 0$ , and a fluctuating force  $F(t)$ , representing the unceasing impacts of the fluid molecules on the particle. The fluctuating force is

considered to be an external force, and is called the Langevin force. In the absence of a potential, the Brownian particle is said to be 'free'. In the Langevin model, the friction force  $\gamma$  and the fluctuating force  $F(t)$  represent two consequences of the same physical phenomenon (namely, the collisions of the Brownian particle with the fluid's molecules). To fully define the model, it is necessary to characterize the statistical properties of the random force.

We assume that the average value of the Langevin force vanishes,  $\langle F(t) \rangle = 0$ . The autocorrelation function of the random force,  $g(\tau) = \langle F(t)F(t + \tau) \rangle$  is an even function of  $\tau$ , decreasing over a correlation time. The correlation time is of the order of the mean time interval separating two successive collisions of the fluid's molecules on the Brownian particle. If this time is much shorter than the other characteristic times, such as for instance the relaxation time, we can represent  $g(\tau)$  as a delta function. Most often, it is also assumed, for convenience, that  $F(t)$  is a Gaussian process (normal distribution). All the statistical properties of the Langevin force are then calculable if only its average and its autocorrelation function are given.

Let us assume that an external force is applied to the particle. This force  $F_{ext}(t)$  adds to the random force  $F(t)$ . In the case of OT,  $F_{ext}(t) = k x(t)$ , this means that the restoring force of the optical trap is proportional to the bead displacement from its equilibrium position, the bottom of the trap's potential well.

An analytical solution for the one-dimensional Langevin' equation is known. However, the two(three)dimensional problem is too complex to be analytically solved. Therefore, we present a finite element (FE)-based simulation as a suitable tool for determining values of the parameters that can be compared with the values extracted from the experimental results on PFM.

## II. SIMULATION PROCEDURE

The finite element model of the problem is given in Fig. 1. According to Maxwell fluid model, the viscoelastic material is represented by a purely viscous damper and a purely elastic spring connected in series [7]. Water is pure viscous fluid. Because of that, it is modeled by a dashpot connected with the particle at the one end, and with constrained translational degree of freedom (DOF) at the other end. For symmetric dashpots along the global X and Y directions, COMBIN14 [8] elements are used. COMBIN14 has longitudinal and/or torsional capabilities in one, two, and three dimensional applications. The element is defined by two nodes, a spring constant ( $k$ ) and damping coefficients  $(c_v)_1$  and  $(c_v)_2$ , where the damping coefficient  $c_v$  is given by  $c_v = (c_v)_1 + (c_v)_2 \nu$  ( $\nu$  is the fluid velocity). In these simulations, we used the linear coefficient  $(c_v)_l$ , only. It is equal to the friction coefficient  $\gamma$  given by Stokes' law (for the small spherical bead):  $\gamma = 6\pi\nu R$ , and depends on the shear viscosity  $\nu$  of the fluid and the particle radius  $R$ . The translational displacements along X and Y, at the damper ends, are constrained (X and Y displacements

are zero, green triangles on the Fig. 1).

A thermal force load is applied in the center of the bead. To obtain X and Y components of the thermal force,  $F_X$  and  $F_Y$ , that satisfy the conditions for fluctuating random force, the Latin Hypercube Sampling method from multivariate normal distribution is used (Matlab Statistics toolbox [9]). The size (N) of the generated 2 column matrix sample ( $F_X$ ,  $F_Y$ ) was selected in such a way that corresponds to the length of time interval in which the simulation should be performed.

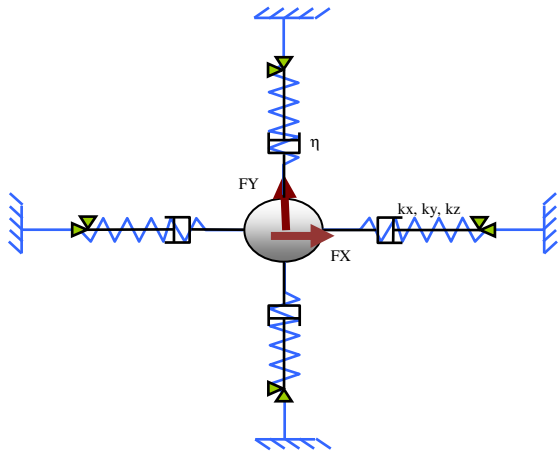
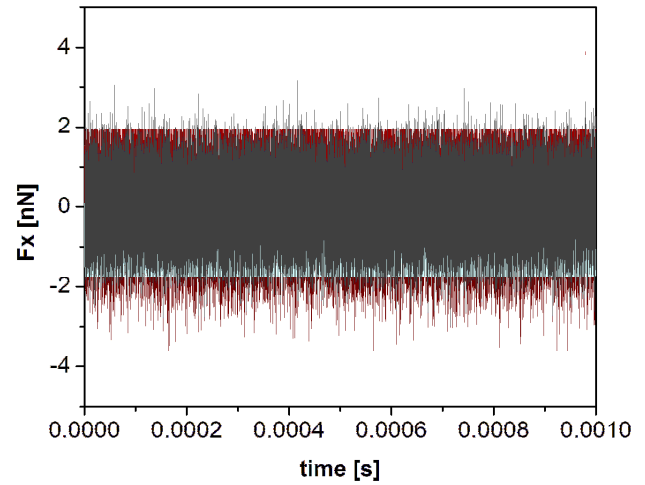


Fig. 1. Illustration of the simulated system. The viscous fluid is represented by a dashpot connected with the particle at the one end, and with constrained translational DOF at the other end. The optical trap is also symbolized by a harmonic spring.

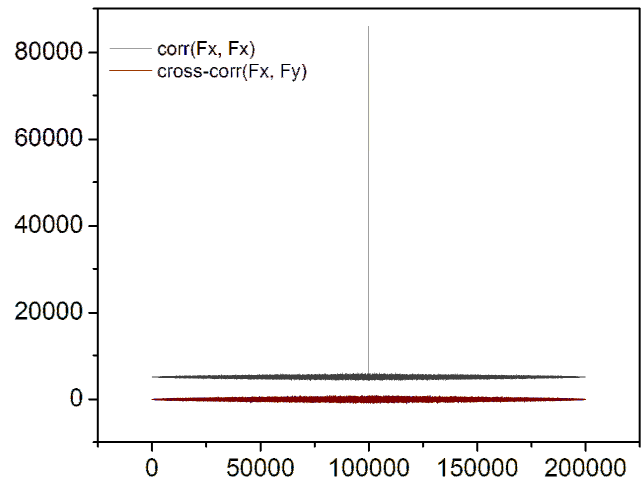
For example: time range 10ns-1ms is divided in 100,000 data points with time step (collision time) of 10 ns. For simplicity, in Fig. 2(a) the X component of the generated thermal force is shown, only, whereas in Fig. 2(b), the  $F_X$  autocorrelation and  $F_X(F_Y)$  cross-correlation sequences (length  $2N-1$ ) are shown. It is obvious that autocorrelation and cross-correlation functions of generated thermal force components are delta and zero functions, respectively. The harmonic potential of optical trap generated by OT is characterized by elastic (spring) constant  $k$ . A two-node element, COMBIN14 with elastic capabilities (spring constant

TABLE I  
THE VALUES OF MATERIAL AND GEOMETRY PARAMETER USED IN SIMULATION

Material Properties	Geometry Properties
silica bead: $EY=70\text{GPa}$ Poisson ratio=0.2 $\rho=2000\text{kg/m}^3$	silica bead: $r=0.5\ \mu\text{m}$
fluid: dynamic viscosity $\nu=10^{-3}\text{Pa}\cdot\text{s}$	$L_{\text{dash-pot}}=15\ \mu\text{m}$ $L_{\text{trap}}=20\ \mu\text{m}$
optical trap: spring constant $k_x=350\ \mu\text{N/m}$ $(k_y=100\ \mu\text{N/m})$	



(a)



(b)

Fig. 2. (a) The  $F_X$  component of random thermal force.  $F_X$  is  $N \times 1$  array ( $N=100,000$ ), generated by Latin Hypercube Sampling method (Matlab Statistics toolbox), (b) The autocorrelation and cross-correlation sequences of  $F_X(F_Y)$  thermal force component given in Figure 2a). The cross-correlation can be neglected compared to autocorrelation delta peak.

defined) is used for modeling optical trap. In the case of symmetric (spatial homogeneity) optical trap, spring constants in both X and Y directions are the same ( $k_x=k_y$ ). The strength of optical trap depends on the spring constant value.

In Table I, the values of material and geometry parameter used in simulation are given.

A structural transient analysis is performed with multiple load steps using DO loop. Time step and number of steps had to be selected to meet the available computer resources. The maximum number of steps is limited to 100,000. Depending on the time range, for the collision time, values of 10, 50 or 100 ns were chosen (time ranges: 10 ns – 1 ms, 50 ns – 5 ms, and 0.1  $\mu\text{s}$  – 10 ms). As the results of simulations, the displacements in both X and Y directions are obtained.

As an example, in Fig. 3 the displacements in both directions (X and Y) for “free” 0.5  $\mu\text{m}$  silica particle in water under thermal fluctuating force, are given.

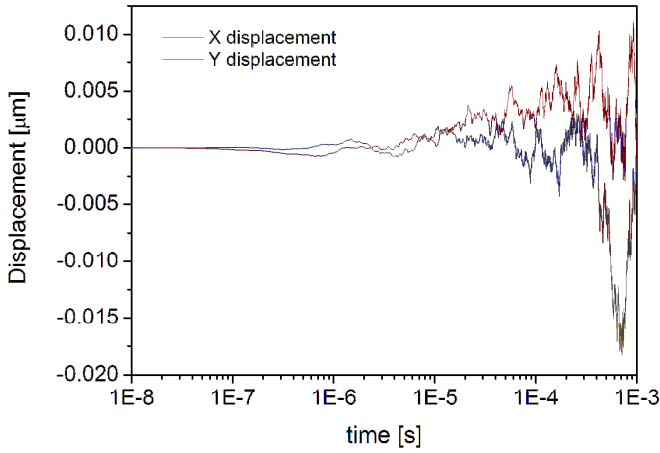


Fig. 3. The results of two dimensional finite element based simulation of Brownian motion of “free” 0.5  $\mu\text{m}$  silica bead in water, under thermal fluctuating force, whose X component (FX) is given in Fig. 2(a). The term “free” means that bead is not optically trapped.

Based on the displacement values, the bead trajectories, as well as the Mean Square Displacements (MSD) are calculated.

$$MSD(\tau) = \langle \Delta r(\tau)^2 \rangle = \langle [r(t+\tau) - r(t)]^2 \rangle$$

where  $r(t)$  is the position of the particle at time  $t$ , and  $\tau$  is the lag time between the two positions. The average  $\langle \dots \rangle$  designates a time-average over  $\tau$ .

### III. RESULTS AND DISCUSION

The simulations under different load conditions are performed:

- Thermal fluctuation of the silica bead in water – without optical trap
- Thermal fluctuation of the silica bead in water – with a symmetric optical trap
- Thermal fluctuation of the silica bead in water – with an asymmetric optical trap

From Brownian trajectories of both “free” silica bead and silica bead trapped by OT, given in Fig. 4 it is obvious that volume exploited by bead is determined by strength of the optical trap. Optical trap is homogeneous,  $k_x = k_y$ .

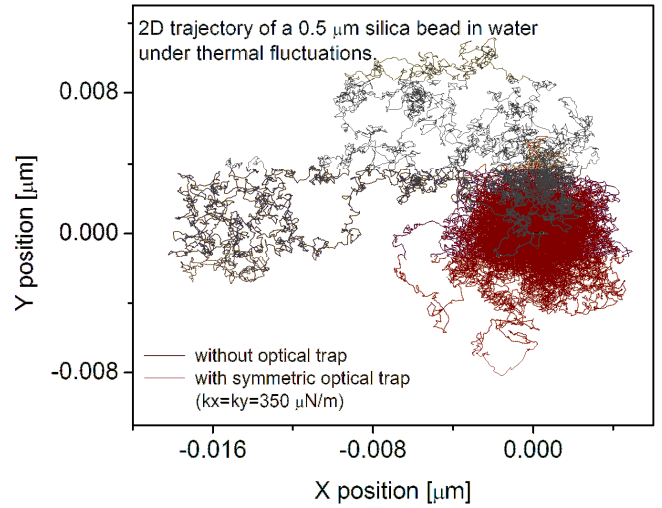


Fig. 4. Two-dimensional trajectories of a 0.5  $\mu\text{m}$  “free” (gray line, top and left) and “trapped” (red line, right) silica bead in water under thermal load force. The spring constants of optical trap in both directions are the same,  $k_x = k_y$  (symmetric optical trap).

Fig. 5(a) shows MSD of “free” bead as a function of time over four decades. Two regimes of the particle motion can be observed, ballistic ( $t < 0.1 \mu\text{s}$ ) and diffusive at  $t > 0.1 \mu\text{s}$ . The slope of the simulated MSD curve at short time scale is double that of the MSD curve at long scale in the log-log plot. At very short time scale, MSD is predicted to be proportional to  $\frac{k_B T}{m^*} t^2$  (ballistic regime).  $m^*$  is an effective mass, by which the hydrodynamic memory effect can be modeled. At the long time scale the MSD increases linearly in time (diffusive regime). Fig. 5(b) displays in more details the Brownian motion at long-time scale in linear-linear plot. The simulated curve is fitted with a linear equation ( $y = a + b \cdot x$ ), and the value of slope  $b$ , 1.9134 is obtained. From the slope value, the value of diffusivity  $D$  of  $4.78 \mu\text{m}^2/\text{s}$  is calculated. That is the accepted value for the viscosity of water at room temperature (Table II). MSD versus  $t$ , at short time-scale is shown in detail in Fig. 5(c)). This curve is fitted with an Allometric2 equation ( $y = a + b \cdot x^c$ ). In the script box the values of the equation parameters are given ( $c = 1.963$ ,  $b = 3.47E6 \mu\text{m}^2/\text{s}^2$ ). The value of  $m^*$  can be estimated based on the value of parameter  $b$ . The value of parameter  $c$ , obtained by fitting confirms the quadratic dependence MSD( $t$ ).

The influence of optical trap symmetry on the Brownian trajectory of 0.5  $\mu\text{m}$  silica bead in water is shown in Fig. 6. These trajectories are simulated over five orders of magnitude in timescale from 50 ns to 5ms (time of correlation is 50 ns).

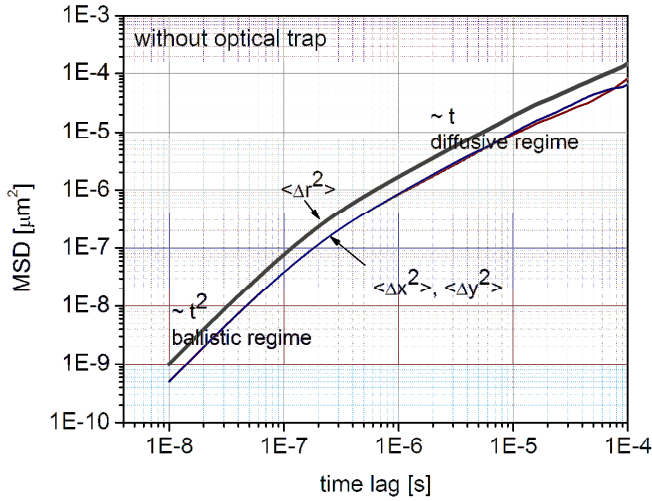


Fig. 5(a). The MSD of a 0.5  $\mu\text{m}$  silica sphere in water. At long time plot ( $t > \tau_p \sim 0.1 \mu\text{s}$ ) the slope of MSD is  $\sim 1$  in log-log scale (diffusive regime), while at short time scale ( $t < \tau_p$ ) the slope of MSD is  $\sim 2$  in log-log plot (ballistic regime).

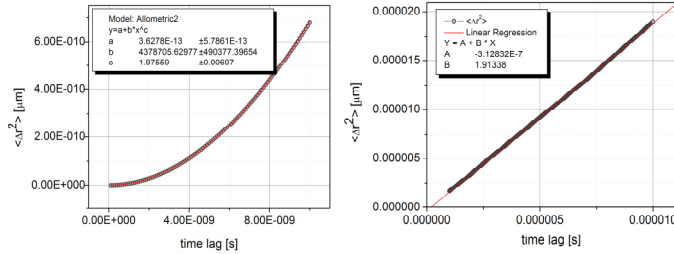


Fig. 5(b). The MSD of a 0.5  $\mu\text{m}$  silica sphere in water at short time-scale given in details.  $\langle \Delta r^2 \rangle$  is fitted with Allometric2 curve  $a+b*t^c$ , and the power  $c$  obtained by fitting is  $\sim 2$ , that is characteristic of ballistic motion.

Fig. 5(c). The MSDs of a 0.5  $\mu\text{m}$  silica sphere in water at long time scale shown in details.  $\langle \Delta r^2 \rangle$  is fitted with linear curve  $a+b*t$ , and the slope  $b$  obtained by fitting is  $\sim D$ , where  $D$  is the diffusion coefficient.

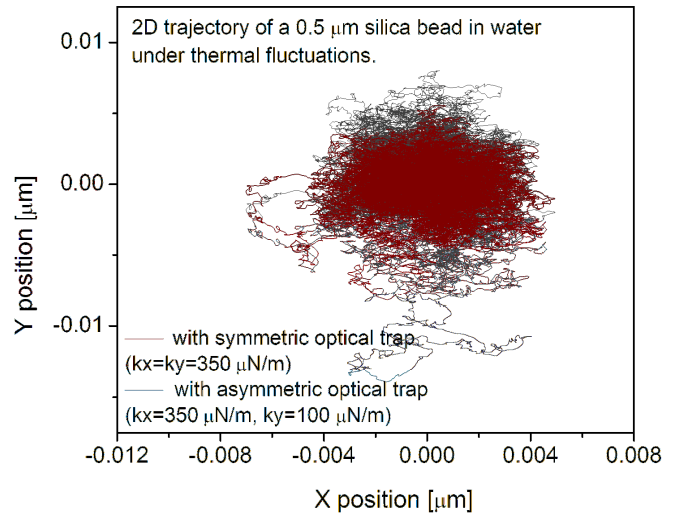


Fig. 6. Two-dimensional trajectories of a 0.5  $\mu\text{m}$  silica bead in water under thermal load force, when bead is trapped by symmetric optical trap,  $k_x=k_y=350 \mu\text{N/m}$  (—), and asymmetric optical trap,  $k_x=350 \mu\text{N/m}$ ,  $k_y=100 \mu\text{N/m}$  (---).

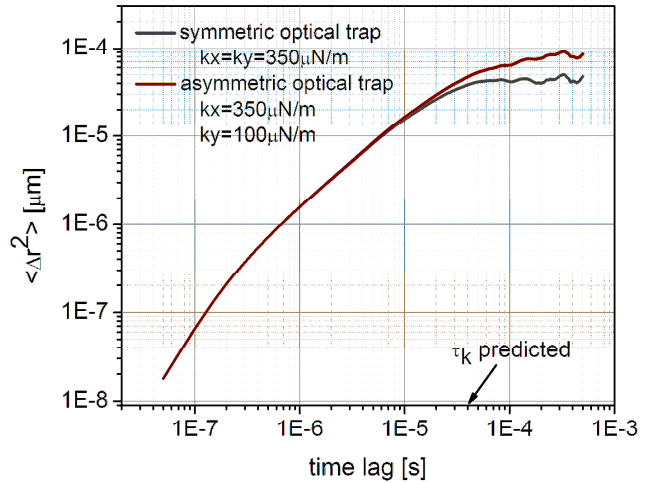


Fig. 7. The MSD of a 0.5  $\mu\text{m}$  trapped silica sphere in water: (—) symmetric ( $k_x=k_y$ ), (---) asymmetric optical trap. After time  $\tau_k$ , the MSD reaches the plateau. The value of plateau depends on the spring constant of the trap.

The Fig. 7 shows that MSD in the case of optically trapped bead increase and then reach the plateau determined by optical trap strength. In the case of symmetrically trapped bead, the MSD reaches the plateau around  $\tau_k = 0.05 \text{ ms}$  (the predicted value of  $\tau_k$  is 0.03 ms, Table II). The values of MSD on the plateau is about  $2.2 \times 10^{-5} \mu\text{m}^2$ , that is in good agreement with theoretically predicted value  $\frac{2k_B T}{k}$  (Table II), where  $k$  is the spring constant of the optical trap. In the case of asymmetric optical trap ( $k_x=350 \mu\text{N/m}$ ,  $k_y=100 \mu\text{N/m}$ ), x-position MSD reaches plateau around 0.05 ms, while y-position MSD (and therefore  $\langle \Delta r^2 \rangle$ ) continues to grow (Fig. 7).

#### IV. CONCLUSION

We used a very simple Maxwell model to investigate the influence of the different parameter of the model (geometry, material properties..) on the Brownian motion of a silica bead

TABLE II  
COMPARISON OF THE VALUES OF PARAMETERS THAT CHARACTERIZE THE BROWNIAN MOVEMENT OF BEAD IN WATER, UNDER THERMAL FLUCTUATION

Parameter	Value obtained by theoretical prediction	Value calculated from the results of simulations
$\tau_p = \frac{m}{\gamma}$	0.1 $\mu\text{s}$	0.08 $\mu\text{s}$
$\tau_k = \frac{\gamma}{k}$	0.027 ms	0.03 ms
Diffusion coefficient $D = \frac{k_B T}{\gamma}$	0.446 $\mu\text{m}^2/\text{s}$	0.478 $\mu\text{m}^2/\text{s}$
MSD plateau (in the case of trapped bead) $\frac{2k_B T}{k}$	2.36E-5 $\mu\text{m}^2$ ( $k=350 \mu\text{N/m}$ ) 8.28E-5 $\mu\text{m}^2$ ( $k=100 \mu\text{N/m}$ )	2.2E-5 $\mu\text{m}^2$ ( $k=350 \mu\text{N/m}$ ) 8E-5 $\mu\text{m}^2$ ( $k=100 \mu\text{N/m}$ )

in water under thermal fluctuating force. The parameters we can change are: the spring constants of optical trap, the bead radius, and the fluid viscosity. From Table II, it is obvious that the results of simulations are in good agreement with the theoretical predictions. The main advantage of the FE based modeling and simulation is that it can consider two(three) dimensional problem for which there is no analytical solution. An analytical solution is almost impossible to find, because the interaction of variables is not known. By changing the values of parameters in the simulation, and comparing the results with the experimental ones, the value of fluid dynamic viscosity can be obtained, if the radius of the probe, and temperature are known. Also, the FE based simulation allows to specify how the variables change with temperature, frequency... In this way it is possible to make conditions close to real experimental conditions. The main disadvantage of this simple model is that viscous fluid can be modeled as a dashpot with friction coefficient  $\gamma$ , in the case of small spherical particle only (Stokes law). If we have a probe of some other geometry, one of the more complicated modeling approaches must be used: solid modeling – where the surrounding medium is meshed with a finite element that supports the viscoelastic properties of materials given in terms of Prony series, or FLOTRAN analysis with Arbitrary Lagrangian – Eulerian (ALE) formulation for moving domains. By using some of these approaches, the influence of surrounding fluid would be more accurately included in the simulation. However, these

approaches make the problem very complex, because besides the load force that is complex enough, we introduce a very complex model of the surrounding fluid. In such a way, the simulations became very demanding. The authors' intention is to continue work in these directions.

#### REFERENCES

- [1] E.-L. Florin, A. Pralle, J. K. Heinrich Horber, E. H. K. Stelzer "Photonic Force Microscope Based on Optical Tweezers and Two-Photon Excitation for Biological Applications", *Journal of structural biology* 119, 202–211, 1997.
- [2] A. Ashkin, J. M. Dziedzic, J. E. Bjorkholm, S. Chu, "Observation of a single-beam gradient force optical trap for dielectric particles", *Opt. Lett.* 11, 288, 1986.
- [3] S. Jeney, F. Mor, R. Koszali, L. Forro, and V. Moy, "Monitoring ligand-receptor interactions by photonic force microscopy", *Nanotechnology*, 21, 255102(8pp), 2010.
- [4] S. Jeney, E.-L. Florin and J.K.H. Horber, "Use of Photonic Force Microscopy to study single-motor-molecule mechanics", *Kinesin Protocols, I. Vernos*, (Humana Press, Totowa, NJ, 2000) pp.91-107.
- [5] T. Li, S. Kheifets, D. Medellin, M. G. Raizen, "Measurements of the instantaneous velocity of a Brownian particle", *Science*, Vol 328, 1673-1675, 25 June 2010.
- [6] R. Huang, I. Chavez, K. M. Taute, B. Lukic, S. Jeney, M. G. Raizen and Ernst-Ludwig Florin, "Direct observation of the full transition from ballistic to diffusive Brownian motion in a liquid", *Nature Physics*, 27 March 2011, doi:10.1038/NPHYS1953
- [7] M. Grimm, S. Jeney, T. Franosch, "Brownian motion in a Maxwell fluid", *Soft Matter*, 7, 2076-2084, 2011, doi:10.1039/c0sm00636j
- [8] ANSYS Release 12.1
- [9] Matlab Release 2007.